Polymer Chemistry

Synthesis of a Soluble Adenine-Functionalized Polythiophene through Direct Arylation Polymerization and its Fluorescence Responsive Behavior

Journal:	*Polymer Chemistry*
Manuscript ID	PY-ART-07-2019-001142.R1
Article Type:	Paper
Date Submitted by the Author:	08-Nov-2019
Complete List of Authors:	Sabury, Sina; University of Tennessee Knoxville Collier, Graham; Georgia Institute of Technology, Ericson, M.; Oak Ridge National Laboratory Kilbey, S.; University of Tennessee Knoxville

Synthesis of a Soluble Adenine-Functionalized Polythiophene through Direct Arylation Polymerization and its Fluorescence Responsive Behavior †

Sina Sabury[a], Graham S. Collier[a,b], M. Nance Ericson[c], S. Michael Kilbey II[a,d]*

[a]Department of Chemistry, University of Tennessee, Knoxville, Tennessee 37996, United States

[b]School of Chemistry and Biochemistry, School of Materials Science and Engineering, Center for Organic Photonics and Electronics, Georgia Tech Polymer Network, Georgia Institute of Technology, Atlanta, Georgia 30332, United States

[c]Electrical and Electronics Systems Research Division, Oak Ridge National Laboratory, Oak Ridge, TN 37831, United States

[d]Department of Chemical and Biomolecular Engineering, University of Tennessee, Knoxville, Tennessee 37996, United States

*E-mail: mkilbey@utk.edu

Abstract

Side chain engineering has been used widely to expand the functionality and enhance the solubility of conjugated polymers, promoting their utility in various applications. Herein, we report synthesizing an adenine-functionalized, thiophene-based alternating copolymer via direct arylation polymerization. This nucleobase-modified, alkyl thiophene-based alternating copolymer was accessed by copolymerization of a Boc-protected, adenine functionalized thiophene monomer 9-(6-(2,5-dibromothiophen-3-yl)hexyl)-9H-purine-6-amine) ($\mathbf{T_{Ad}}$), with 3,3',3",4'-tetrahexyl-2,2':5',2"-terthiophene, ($\boldsymbol{t}\mathbf{T_{4h}}$). Quantitative post-polymerization deprotection of Boc groups results in the adenine bearing alternating copolymer ($\mathbf{T_{Ad}}$-$\boldsymbol{t}\mathbf{T_{4h}}$), which is soluble in common organic solvents due to steric hindrance-induced flexibility of the $\boldsymbol{t}\mathbf{T_{4h}}$ comonomer allowing structure-property relationships to be established. In comparison to the unfunctionalized analogue, interchain hydrogen bonding through the adenine functionality enhances the packing of the copolymer, resulting in a ~70 °C increase in the glass transition temperature. Furthermore, the improved solubility of the copolymer and capacity for strong metal ion binding by the nucleobase

leads to dramatic fluorescence quenching (> 90%) upon the addition of Cu^{2+} ions, which is also reflected in a high Stern-Volmer constant of 1.28×10^4 M^{-1}. The fluorescence emission is recovered almost completely after washing the copolymer solution with EDTA-disodium salt aqueous solution. These findings demonstrate the viability of synthesizing soluble, fully conjugated copolymers with nucleobase functionality via direct arylation polymerization, as well as the influence of the hydrogen bonding nucleobase on thermal, optical, and metal-ion sensing properties.

Introduction

Side chain engineering is used extensively to manipulate optoelectronic or physical properties of conjugated polymers.[1-6] Solubilizing side chains minimize the tendency of conjugated polymers to aggregate or crystallize, which are behaviors driven by π-π stacking interactions and backbone rigidity.[7] In addition, side chain functionality also can be used to manipulate optoelectronic properties. Electron donating or electron withdrawing groups that are in close proximity to the backbone typically will change the HOMO and LUMO of the conjugated polymer.[3, 8-10] Functional groups at the terminus of the side chain tend to influence electronic properties of the conjugated polymer indirectly by influencing the morphology, backbone planarity, or interchain interactions.[11-13] One useful strategy for controlling morphology while enhancing thermal stability and solvent resistivity of bulk heterojunction (BHJ) organic photovoltaics (OPVs) or organic field effect transistors (OFETs) is to integrate functional motifs into side chains that interact through hydrogen bonding interactions.[14-17] For example, Stupp and coworkers compared the OPV performance of two diketopyrrolopyrrole-based, donor-type small molecules, where the only difference in design was the presence of either amide or ester functionalities at the same location in the side chains.[16] Although both molecules showed similar

optoelectronic properties, OPVs based on the amide-functionalized molecule exhibited power conversion efficiencies (PCEs) that were 50% higher than OPVs made with the ester-functionalized molecule. They attributed the increase in PCE to the self-complementary hydrogen bonding between amide groups in the side chains. These non-bonded, pair-wise intermolecular interactions compete with π-π stacking, resulting in a morphology with a smaller domain size.[16] Additionally, Yao et al. showed interchain packing order of a diketopyrrolopyrrole copolymer is improved upon introduction of urea functionality in the side chain. The hydrogen bonding ability of urea groups promoted lamellar stacking that enhanced hole mobility.[18] The benefits of hydrogen bonding (H-bonding) motifs in the side chains of conjugated polymers extend beyond improving the performance of OPVs or OFETs. A variety of studies have shown that H-bonding groups in conjugated polymers engenders their use in applications such as optical DNA sensors or ion detectors.[19-27] In total, these studies highlight the utility of hydrogen bonding engineered into side chains as means to expand or improve the performance of conjugated polymers.

Nucleobases, which are used by nature and offer complementary hydrogen bonding motifs, have been explored extensively as side chain functionality in polymeric materials, especially in non-conjugated polymers.[28-33] Nucleobase-functionalized polymers have shown promise in numerous applications, including polymer adhesives, self-healing materials, donor and acceptor compatibilization, and sensors.[32, 34, 35] In the realm of conjugated polymers, a promising improvement in hole transport properties was observed by Cheng et al., who synthesized a uracil-functionalized polythiophene via oxidative polymerization and used this material as a hole transport layer.[15] Similarly, Yang et al. fabricated an organic field-effect transistor (OFET) device based on thymine-functionalized diketopyrrolopyrrole copolymer. They observed that hydrogen bonding between thymine groups located at the terminus of the side chains created interchain

connectivity, which increased the charge mobility of the conjugated polymer. In the same study, the ability of metal ions, such as Pd^{2+} or Hg^{2+}, to coordinate with thymine was used as a basis to tailor the selectivity of an OFET-based gas sensor toward gases such as CO and H_2S.[36] This ability of metal ions to form strong coordinate bonds with nucleobases is also the basis of solution detection of metal ions.[37] In the realm of conjugated polymers, Tang et al. observed that the binding of Hg^{2+} with a thymine-functionalized analog of poly(3-hexylthiophene) resulted in fluorescence quenching.[26] Similarly, Xing et al. demonstrated that the fluorescence of a thymidine-functionalized polythiophene was quenched upon addition of Cu^{2+}.[19]

Although nucleobase functionalities provide a way to enhance the properties and improve the performance of conjugated polymers, there remains significant challenges related to synthetic methodology and solubility of nucleobase-functionalized conjugated polymers. For example, adenine-, thymine-, and uracil-functionalized polythiophenes have been synthesized via oxidative polymerization of 3-(ω-[nucleobase]hexyl)thiophene, which requires stoichiometric amounts of iron (III) chloride for polymerization and generally results in a polymer with limited solubility.[15, 19, 26, 38] Iron (III) chloride is a harmful and highly corrosive, and as shown by Holdcroft et al. and Sariciftci et al., even intense post-polymerization purification leaves behind substantial amounts of iron compounds (~1000 ppm).[39, 40] While nucleobase-functionalized conjugated polymers are conceptually attractive for their utility in biological applications, the presence of these metal impurities may limit their use in such contexts.[41] Additionally, nucleobases are known to have limited solubility in organic solvents due to their strong hydrogen bonding and π-stacking. The adenine-functionalized poly(3-alkylthiophene) reported by Cheng et al. was found to be insoluble in most organic solvents, even at molecular weights as low as M_n = 2.8 kg/mol.[38, 42] These

limitations motivates efforts to explore more benign synthetic methodologies as well as to develop useful routes to maintain functionality while offering improved solubility.

Recently, direct arylation polymerization, which is commonly referred to as "DArP", has become a robust methodology for synthesizing conjugated polymers using diverse comonomer building blocks.[43, 44] DArP is considered a green, less toxic polymerization method for two reasons. First, the need for organometallic comonomers is eliminated in DArP due to direct activation of (hetero)aromatic hydrogens, which simplifies monomer synthesis and reduces the number of synthetic steps.[43-48] Second, because DArP does not require organometallic comonomers, toxic byproducts, such as organotin species that are produced in stoichiometric amounts in Stille cross-coupling polymerizations, for example, are no longer generated. As an illustrative example of these advantages, for example, Reynolds et al. showed that dioxythiophene-based conjugated polymers synthesized by DArP contain 100 times less catalyst impurities compared to those made using oxidative polymerization.[49] While DArP has been used to synthesize various conjugated polymers, especially polythiophenes, its functional group tolerance and more specifically its potential with nucleobase-functionalized materials remains unexamined.

Herein, we report the synthesis of a soluble adenine-functionalized, alternating polythiophene copolymers via DArP. Within this effort, the effect of the electron-rich and chelating adenine functionality on the polymerization is studied in detail. We describe the impact of adenine-functionality as a hydrogen bonding active and highly chelating group on photophysical properties, and thermal transitions. Additionally, chelation-induced fluorescent quenching upon binding copper ions with adenine and its reversibility are examined. This work expands the synthetic toolbox for nucleobase-functionalized conjugated polymers, while also providing insight into functional group tolerance of DArP, exemplifying the importance of monomer design and

side chain engineering on the synthesis, solubility, and properties of these nucleobase-functionalized conjugated polythiophenes.

Results and Discussion

Monomer and Polymer Syntheses

Synthetic details as well as results of characterization of all intermediate compounds is relegated to the *Supplementary Information*. As highlighted in Scheme 1, lithium-halogen exchange was used to produce 3-(6-bromohexyl)thiophene from 3-bromothiophene in 70% yield.[50, 51] After purification, the resulting 3-(6-bromohexyl)thiophene was brominated using *N*-bromosuccinimide (NBS) to generate 2,5-dibromo(3-(6-bromohexyl)thiophene in 75% yield.[51] Bromination preceded addition of adenine to avoid bromination of adenine at the C-8 position.[52] Finally, adenine-functionality was introduced at the terminus of the side chain functionality under alkylation conditions, as described by our group[53, 54] and others.[52, 55, 56] While this results in a mixture of N-7 and N-9 attachment,[57] the N-9 isomer, 9-(6-(2,5-dibromothiophen-3-yl)hexyl)-9H-purine-6-amine) (**M1**), was isolated by column chromatography, resulting in an overall yield of 55%. The adenine-functionalized monomer featuring N-9 attachment was chosen for polymerization due to its similarity to adenosine as well as its ability to participate in multi-dentate hydrogen bonding with other nucleobases, such as thymine.[57] The structure of the adenine-functionalized thiophene (**M1**) was confirmed by 2D multiple bond correlation gHMBC NMR spectroscopy, and relevant correlations are shown in Figure S7.

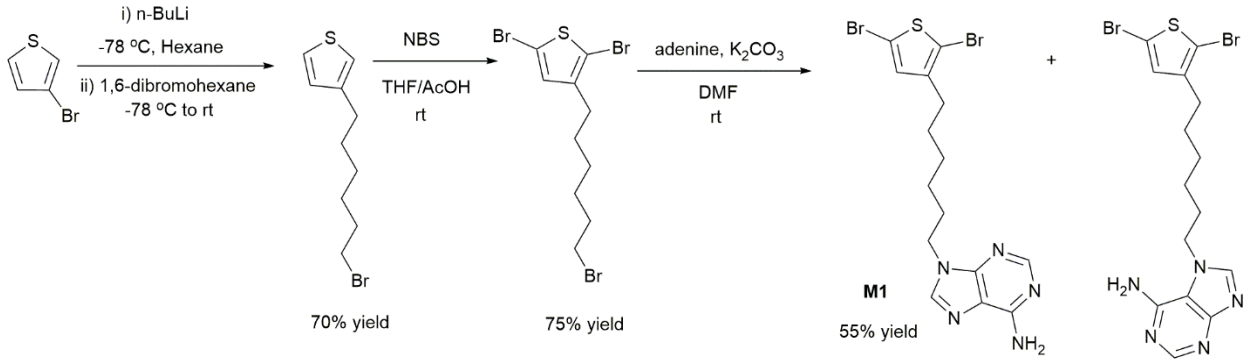

Scheme 1. Synthetic pathway used to synthesize the adenine-containing dibromo monomer **M1**.

Initial efforts to copolymerize **M1** with 3-hexylthiophene by applying conditions reported extensively in the literature for the DArP of thiophenes[43, 44, 48, 58, 59] were unsuccessful. (See Scheme S2 of the ESI.) We hypothesized that adenine may interfere with polymerization in two possible ways: i) The C-H bond at the C-8 position of the purine scaffold may be activated,[60] creating a stoichiometric imbalance that inhibits the step-growth polymerization, or ii) the nucleobase may ligate the palladium catalyst,[37] thereby inhibiting the catalyst from participating in the catalytic cycle. A set of test polymerizations were performed to differentiate between these two effects. First, a catalytic amount of *N*-hexyl adenine (0.04 equiv.) was added to a copolymerization properly constituted with 2,5-dibromo-3-hexylthiophene and 3-hexylthiophene. (See Scheme S3.) If the issue were stoichiometric imbalance due to activation of the C-H bond at C-8, this test polymerization would result in low molecular weight polymer; however, if the second cause –disruption of catalytic activity– was operative, the polymerization would not proceed. As detailed in Table S1, reactions were performed in both polar and nonpolar solvents using catalysts that include $Pd(OAc)_2$, Hermann-Beller's catalyst, $Pd(PPh_3)_4$, and $Pd_2(dba)_3$ with appropriate ligands, bases and proton shuttles. Regardless of catalyst, solvent, temperature, and auxiliary ligand, no polymer was observed when a catalytic amount of *N*-hexyl-adenine was present. Specific reaction conditions and outcomes are documented as entries 1-14 in Table S1. In addition,

DArP using Fagnou conditions in the presence of excess Cu^{2+} (provided by CuI) as a sacrificial complex-forming ion that can coordinate with adenine groups was attempted. (See entries 15 and 16 in Table S1.) In this situation, an oligomer (M_n = 2,000 g/mol) was formed at low yield (15%) when bulky phosphine ligands were added. This screening study suggests that adenine is strongly binding with the palladium metal center, thereby deactivating the catalyst. This conclusion is consistent with the ability of nucleobases to bind with various metal ions, which has been reported widely.[61-64]

Therefore, a second series of test polymerization were run, this time using a *tert*-butyloxycarbonyl (Boc) protected *N*-hexyl-adenine (0.04 equiv.) as an additive in the reaction mixture. In this situation, the DArP of 2-bromo-3-hexylthiophene (which is shown in Scheme S5) produced P3HT at 45% yield with a number-average molecular weight M_n = of 5.9 kg/mol and dispersity of $Đ$ = 1.68. These studies indicate that it is necessary to protect the amine functional group of adenine to enable a successful polymerization via DArP.

These test polymerization results prompted the synthesis of the amine-protected dibromo monomer, **M2**, which as shown in Scheme 2, has two Boc protecting groups. The structure of the amine-protected dibromo monomer is confirmed by ^{1}H, ^{13}C, and 2D gHMBC NMR spectroscopy, which are presented in Figures S8, S9, and S10, respectively. In addition and as shown in Figure 1, successful protection of the amine is evident from the change of chemical shifts corresponding to the C-2 and C-8 protons of adenine. Specifically, when **M1** is transformed to **M2**, the C-2 proton shifts from 8.35 ppm to 8.77 ppm, and the C-8 proton shifts from 7.77 ppm to 8.00 ppm due to the addition of electron withdrawing Boc groups.

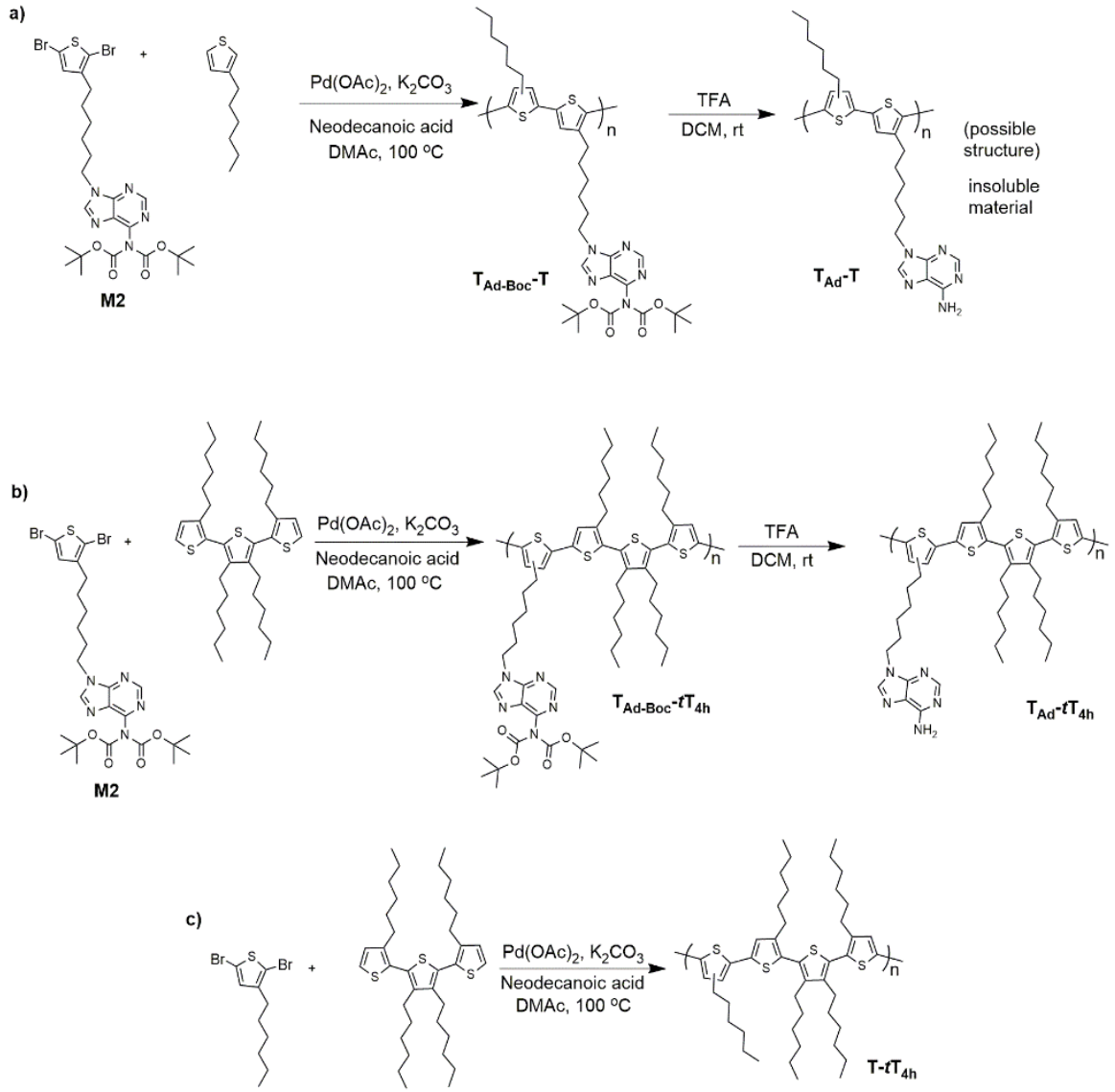

Scheme 2 Synthesis of Boc-protected copolymers (a) $\mathbf{T_{Ad\text{-}Boc}\text{-}T}$, (b) $\mathbf{T_{Ad}\text{-}\textit{t}T_{4h}}$, and (c) the non-functionalized homologue, $\mathbf{T\text{-}\textit{t}T_{4h}}$ via direct arylation polymerization as well as Boc deprotection conditions for $\mathbf{T_{Ad\text{-}Boc}\text{-}T}$ and $\mathbf{T_{Ad}\text{-}\textit{t}T_{4h}}$.

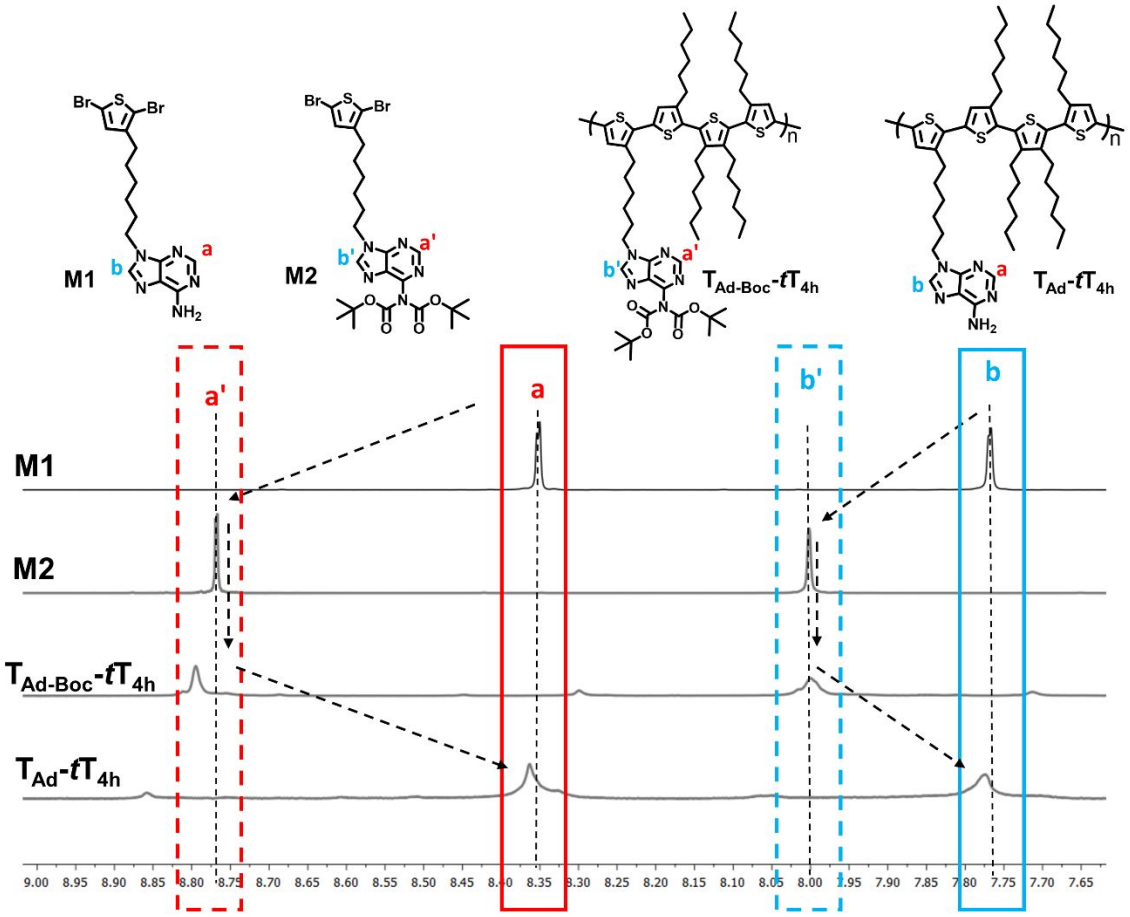

Figure 1. Overlay of the aromatic regions of ^{1}H NMR spectra acquired for **M1**, **M2**, $\mathbf{T_{Ad\text{-}Boc}}$-$\boldsymbol{t}\mathbf{T_{4h}}$, and $\mathbf{T_{Ad}}$-$\boldsymbol{t}\mathbf{T_{4h}}$. Comparison of the spectra shows that the C2 and C8 protons shift downfield (upfield) when adenine is Boc-protected (deprotected), and peak widths broaden and shift slightly upon polymerization.

By using conditions described by Thompson and coworkers[58, 59] as optimized conditions for DArP of thiophene-based monomers, P3HT was synthesized with 68% yield with a number-average molecular weight M_n = 35.0 kg/mol and dispersity $Đ$ = 2.10. Therefore, these conditions were applied to the DArP of **M2** with other comonomers. As shown in Scheme 2a, direct arylation polymerization of **M2** with 3-hexylthiophene as the complementary comonomer was successful using $Pd(OAc)_2$ (0.06 equiv.) as the catalyst, dimethylacetamide (DMAc) as solvent, K_2CO_3 as the base, and neodecanoic acid as the proton shuttle. The resulting alternating regiorandom copolymer

comprised of Boc-protected thiophene and 3-hexylthiophene repeating units, which are abbreviated as $\mathbf{T_{Ad\text{-}Boc}}$-**T**, with subscripts designating the nature of the side chain, was purified and isolated as a green solid in 56% yield with M_n = 6.9 kg/mol and $Đ$ = 1.37. (See Figure S23 and Figure S24 for GPC trace and ^{1}H NMR spectrum, respectively.) Deprotection of the Boc functionality resulted in an insoluble dark-yellow solid. This drastic change in solubility after cleaving the protecting groups is attributed to strong interchain hydrogen bonding interactions between adenine groups, with the insolubility exacerbated by the lack of solubilizing alkyl side chains, which was also reported by Cheng and coworkers.[38, 42]

In an effort to improve the solubility of adenine-containing conjugated polymers, the comonomer 3,3',3'',4'-tetrahexyl-2,2':5',2''-terthiophene (***t*T$_{4h}$**) was synthesized. Here the key design element is additional solubilizing side chains within a bulkier complementary comonomer. In comparison to 3-hexylthiophene, this monomer contains more hexyl side chains per thienyl ring, which is expected to reduce main chain rigidity[65-67] and effectively dilute[68] the number of network-forming adenine groups throughout the copolymer, thereby improving copolymer solubility. As described in the *Supplementary Information*, ***t*T$_{4h}$** was synthesized in 80% yield using Suzuki cross-coupling between 2,5-dibromo-3,4-dihexyl-thiophene and 3-hexylthiophene-2-boronic acid pinacol ester in toluene and water biphasic system at 95 °C. (See Figures S11-S14.) Direct arylation polymerization of **M2** with ***t*T$_{4h}$** (Scheme 2b) using optimized DArP conditions[58, 59] resulted in $\mathbf{T_{Ad\text{-}Boc}}$-***t*T$_{4h}$** with M_n = 7.0 kg/mol, $Đ$ =2.01 (72% yield). Regiorandomness of this alternating copolymer, similar to $\mathbf{T_{Ad\text{-}Boc}}$-**T**, comes from nature of AA plus BB step-growth polymerization. However, intrinsic symmetry of the ***t*T$_{4h}$** monomer ensures that the ***t*T$_{4h}$**-containing copolymers has one head-tail connection and one tail-tail connection in each dyad, regardless of polymerization conditions. Acid catalyzed deprotection of Boc groups using

trifluoroacetic acid (TFA) produced the alternating copolymer designated as $\mathbf{T_{Ad}}$-*t*$\mathbf{T_{4h}}$ (M_n = 7.0 kg/mol, $Đ$ =1.82), which was soluble in common organic solvents such as THF and chloroform. GPC traces of $\mathbf{T_{Ad\text{-}Boc}}$-*t*$\mathbf{T_{4h}}$ and $\mathbf{T_{Ad}}$-*t*$\mathbf{T_{4h}}$ are unimodal (Figure S25) and full ^{1}H NMR spectra of the Boc-protected and deprotected copolymers are presented as Figures S26 and Figure S27, respectively. As a result of the improved solubility, extensive structural characterization of the adenine-functionalized copolymer $\mathbf{T_{Ad}}$-*t*$\mathbf{T_{4h}}$ is possible. As shown in Figure 1, ^{1}H NMR spectroscopy suggests that amine groups remained protected during polymerization and the Boc deprotection is quantitative. Specifically, chemical shifts corresponding to protons at the C-2 and C-8 positions of adenine show retention of Boc functionality during polymerization for both $\mathbf{T_{Ad\text{-}Boc}}$-**T** and $\mathbf{T_{Ad\text{-}Boc}}$-*t*$\mathbf{T_{4h}}$. Following deprotection of $\mathbf{T_{Ad\text{-}Boc}}$-*t*$\mathbf{T_{4h}}$ with TFA, upfield shifts are observed for protons at the C-2 and C-8 positions of the adenine, which confirms complete deprotection.

To examine the effect of adenine side chain functionality on thermal and optical properties, a non-functionalized homologue, identified as **T**-*t*$\mathbf{T_{4h}}$, was synthesized from *t*$\mathbf{T_{4h}}$ and 2,5-dibromo-3-hexylthiophene using optimized DArP conditions (Scheme 2c). This copolymer was produced as a viscous paste in 71% yield and found to have a M_n = 8.5 kg/mol and Đ = 1.64. (See Figure S28 and Figure S29 for GPC trace and ^{1}H NMR spectrum.)

Thermal Characterizations of Copolymers

Thermogravimetric analysis (TGA) was used to assess the thermal stability of $\mathbf{T_{Ad}}$-*t*$\mathbf{T_{4h}}$ and **T**-*t*$\mathbf{T_{4h}}$. As shown in Figure S30a, **T**-*t*$\mathbf{T_{4h}}$ has a decomposition temperature (T_d), which is defined as the temperature at which a 5% weight loss is registered, of 397 °C. This T_d and ultimate weight of ~46 wt% agree with values reported for poly(alkylthiophenes).[69] Alternatively, $\mathbf{T_{Ad}}$-*t*$\mathbf{T_{4h}}$

exhibits a multi-step degradation, as observed in Figure S30b. $\mathbf{T_{Ad}}$-*t*$\mathbf{T_{4h}}$ has a T_d of 171 °C, which is the first degradation event, and a second decomposition occurs at ~ 410°C (where the mass loss is 18%). The first degradation event is attributed to the decomposition of the purine structure in the side chain, which agrees with our previous studies of purine-based copolymers and donor-acceptor chromophores.[53, 54] The second decomposition is consistent with degradation of the poly(alkylthiophene)s. Other possible thermal transitions such as crystallization and glass transition were investigated using differential scanning calorimetry (DSC). $\mathbf{T_{Ad}}$-*t*$\mathbf{T_{4h}}$ and **T**-*t*$\mathbf{T_{4h}}$ do not show a thermal transition corresponding to crystallization due to their highly flexible backbones. (See DSC curves presented in Figure S31.) However, comparison of the DSC traces clearly shows that adenine and its ability to impart interchain hydrogen bonding significantly affects main-chain flexibility: The glass transition temperature (T_g) of the non-functionalized homologue **T**-*t*$\mathbf{T_{4h}}$ is much lower (T_g = −18 °C) than that of the adenine functionalized $\mathbf{T_{Ad}}$-*t*$\mathbf{T_{4h}}$, which displays a T_g = 52 °C. An increase in T_g due to interchain hydrogen bonding has also been observed in conjugated[15, 70] and non-conjugated[32, 71] nucleobase-functionalized polymers and copolymers.

Optical Properties of Copolymers

Motivated by the possibility of conjugated polymers having site-specific intermolecular recognition via hydrogen-bonding abilities finding applicability in a variety of sensing, optoelectronic, and biological applications, the optical properties of the adenine-functionalized polythiophenes were investigated using absorbance and fluorescence spectroscopies. As illustrated in Figure 2a, UV-vis absorption spectra of $\mathbf{T_{Ad}}$-*t*$\mathbf{T_{4h}}$ and **T**-*t*$\mathbf{T_{4h}}$ in chloroform show an absorbance maximum (λ_{max}^{abs}) at 392 nm and 394 nm, which corresponds to the π-π* transition of a conjugated polythiophene with bulky side chains.[72] The adenine-containing polymer, $\mathbf{T_{Ad}}$-*t*$\mathbf{T_{4h}}$, shows an extra

absorbance transition at 262 nm, which corresponds to the π–π* transition of adenine.[73] The same optical transition was observed for *N*-hexyl-adenine in chloroform (blue trace in Figure 2a). Figures S32 and S33 show that absorbance is linearly dependent on concentration across a concentration range of 0.003-0.05 mg/mL in chloroform, resulting in extinction coefficients of ε = 27.8 $(mg/mL)^{-1}$ cm^{-1} for **T-*t*T$_{4h}$**, and ε = 21.1 $(mg/mL)^{-1}$ cm^{-1} for **T$_{Ad}$-*t*T$_{4h}$** (based on absorbance modes at λ_{max}^{abs}). This indicates good solubility for both polymers. Both copolymers are soluble at higher concentrations, but the absorbance intensity exceeds the detection limit of the spectrophotometer at concentrations >0.05 mg/ml. Additionally, the absence of extra absorbance shoulders attributed to vibronic fine structure likely originates from the regiorandom nature of the copolymers and their excellent solubility.[74]

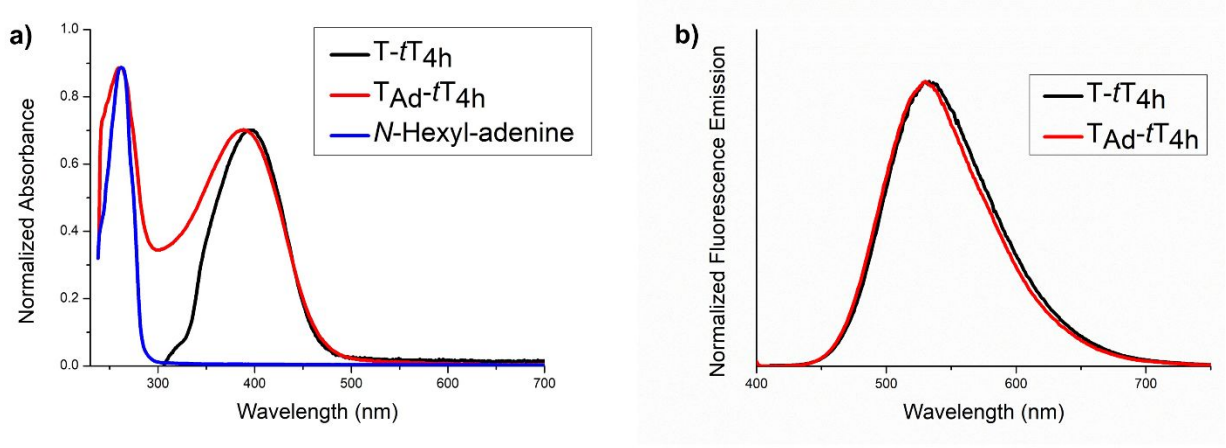

Figure 2. (a) Normalized UV-vis absorbance spectra of **T-*t*T$_{4h}$** (black, 0.01 mg/mL), **T$_{Ad}$-*t*T$_{4h}$** (red, 0.01 mg/mL), and *N*-hexyl-adenine (blue, 50 μM) in chloroform. (b) Normalized fluorescence spectra of **T$_{Ad}$-*t*T$_{4h}$** (red) and **T-*t*T$_{4h}$**(black) in chloroform (0.01 mg/mL).

As shown in Figure 2b, fluorescence spectroscopy measurements show that both **T$_{Ad}$-*t*T$_{4h}$** and **T-*t*T$_{4h}$** have broad and featureless emission profiles, centered around an emission maximum of λ_{max}^{em} = 528 nm and λ_{max}^{em} = 536 nm for **T$_{Ad}$-*t*T$_{4h}$** and **T-*t*T$_{4h}$**, respectively. The similarity of the

emission profiles of $\mathbf{T_{Ad}}$-*t*$\mathbf{T_{4h}}$ and **T**-*t*$\mathbf{T_{4h}}$ suggests that the radiative decay pathways for both polymers mainly originate from the conjugated polythiophene backbone.[75-77] In order to gain more insight of optical properties, fluorescence quantum yields were determined by the comparative method,[54, 78] using Rhodamine 101 in ethanol (+0.01% HCl) as the fluorescence standard (quantum yield, φ = 1.00).[79] The $\mathbf{T_{Ad}}$-*t*$\mathbf{T_{4h}}$ and **T**-*t*$\mathbf{T_{4h}}$ copolymers have similar fluorescence quantum yields of ~0.1, which is comparable to quantum yields reported for poly(alkylthiophenes).[80, 81] Table 1 summarizes the measured optical properties of $\mathbf{T_{Ad}}$-*t*$\mathbf{T_{4h}}$ and **T**-*t*$\mathbf{T_{4h}}$. In addition to similar emission profiles, the nearly identical quantum yield values indicate an absence of alternative decay pathways of the excited state, which suggests that the pendant nucleobase functionality does not interfere with the optical properties of the parent copolymer.

Table 1. Summary of optical properties of $\mathbf{T_{Ad}}$-*t*$\mathbf{T_{4h}}$ and **T**-*t*$\mathbf{T_{4h}}$.

Copolymer	λ_{max}^{abs} (nm)	λ_{max}^{em} (nm)	Stokes Shift (nm)[a]	φ[b]
$\mathbf{T_{Ad}}$-*t*$\mathbf{T_{4h}}$	262, 392	528	136	0.11
T-*t*$\mathbf{T_{4h}}$	394	536	140	0.14

[a]Stokes shifts are calculated as the difference between absorbance and emission maximums.

[b]Quantum yields are calculated using the comparative method.

Both the adenine-functionalized copolymer and the corresponding unfunctionalized copolymer have a large Stokes shift of 136 nm for $\mathbf{T_{Ad}}$-*t*$\mathbf{T_{4h}}$ and 140 nm for **T**-*t*$\mathbf{T_{4h}}$. These Stokes shift values are slightly larger than values reported for regioregular P3HT, which has a Stokes shift of ~130 nm in chloroform[82] but smaller than values of ~150 nm reported by Xu and Holdcroft for regiorandom P3HT in chloroform.[83] In addition, a large Stokes shift, which manifests by minimal overlap of absorbance and emission profiles, minimizes self-quenching and is beneficial for applications including molecular imaging, molecular recognition, and optical sensing.[84-86] Therefore, the large Stokes shift of the $\mathbf{T_{Ad}}$-*t*$\mathbf{T_{4h}}$ copolymer, its inherent solubility, and potential

for molecular recognition through hydrogen bonding motivated fluorescent responsiveness studies.

Fluorescence Quenching Studies

Given the ability of adenine to bind with transition metals and motivated by previous examples where thymine-functionalized polymers interacted with metal ions,[26] we investigated fluorescence responsiveness of $\mathbf{T_{Ad}}$-$\boldsymbol{t}\mathbf{T_{4h}}$ in the presence of a metal ion. $\mathbf{T_{Ad}}$-$\boldsymbol{t}\mathbf{T_{4h}}$ quickly responded to the addition of a copper bromide salt (Cu^{2+}) solution, whereas **T**-$\boldsymbol{t}\mathbf{T_{4h}}$ showed no changes in its fluorescence profile when Cu^{2+} ions were present in solution at 20 μM. (See Figure S35.) In order to evaluate Cu^{2+} detection via fluorescence quenching, the emission profiles of a 0.01 mg/mL solution of $\mathbf{T_{Ad}}$-$\boldsymbol{t}\mathbf{T_{4h}}$ in THF were monitored as a function of [Cu^{2+}]. Noticeable fluorescence quenching occurred in the solution of $\mathbf{T_{Ad}}$-$\boldsymbol{t}\mathbf{T_{4h}}$ at 2×10^{-5} M Cu^{2+} without any shift in λ_{max}^{em}. As shown in Figure 3a, fluorescence intensity of the $\mathbf{T_{Ad}}$-$\boldsymbol{t}\mathbf{T_{4h}}$ decreased with increasing [Cu^{2+}], culminating with a quenching efficiency as high as 91% at [Cu^{2+}] = 5×10^{-4} M. Here, the fluorescence quenching efficiency (Q_{eff}) at $\lambda_{max}^{em}$is calculated using the following expression:

$$Q_{eff} = \frac{I_0 - I(c)}{I_0} \quad (1)$$

In Equation1, I_0 is the fluorescence intensity of the solution in the absence of a quenching reagent and I(c) is the measured fluorescence intensity of the solution in the presence of the quencher (Cu^{2+} for these experiments) at concentration c. As shown in Figure 3b, a linear response is observed for [Cu^{2+}] ranging from 2.0×10^{-5} M to 9.0×10^{-5} M. This is indicative of chelation-induced quenching, which is analyzed by fitting the linear-response region with the Stern-Volmer equation, which is shown in Equation 2.[84, 87, 88]

$$\frac{I_0}{I} = 1 + K_{SV}[\mathrm{Cu}^{2+}] \quad (2)$$

Here, K_{SV} is the Stern-Volmer quenching constant. K_{SV} is related to the propensity of complex formation, here between Cu^{2+} and adenine groups, and it reflects the strength of the association.[89] While fluorescence quenching may occur through formation of non-radiative complexes (static) or chelation-elevated collision between complexes formed (dynamic), the nature of this behavior can only be determined through fluorescence lifetime studies or temperature dependent fluorescence measurements, though the linearity over this concentration range suggests that only one quenching mechanism is governing.[90] While Figure S36 shows that [Cu^{2+}] up to 500 μM were examined, which resulted in >90% quenching efficiency, the Stern-Volmer plot for $\mathbf{T_{Ad}}$-$\boldsymbol{f}\mathbf{T_{4h}}$ only shows linear behavior up to $c = 9 \times 10^{-5}$ M Cu^{2+}. This is reflected in Figure 3b, where fitting yields $K_{sv\,(\mathbf{TAd\text{-}fT4h})} = 1.28 \times 10^4\ M^{-1}$, which is similar to values reported for Cu^{2+} and amine-containing fluorescence probes, such as triphenylamine.[88] At [Cu^2] > 9×10^{-5} M, the concentration dependence changes, suggesting that both static and dynamic quenching contribute in chelation-induced quenching, where the Cu^{2+}-chelated adenine complexes are able to enhance formerly forbidden intersystem crossing or non-radiative decay of the singlet excited state.[19, 87, 89]

Other metal ions, including Cu^+, Fe^{2+}, Fe^{3+}, K^+, and Na^+, were tested to gain more information about nature and selectivity of fluorescence quenching behavior. In these experiments, the concentration of $\mathbf{T_{Ad}}$-$\boldsymbol{f}\mathbf{T_{4h}}$ was fixed at 0.01 mg/mL in THF and metal ion concentrations of 400 μM were used because of solubility issues. Cu^{2+} and Fe^{3+} showed highest quenching efficiencies (78% and 72%, respectively), followed by Fe^{2+}, which showed a lower quenching efficiency (57%) . Other metal ions (Cu^+, K^+, and Na^+) did not affect fluorescence. This is in agreement with intersystem crossing facilitated by paramagnetic ions/atoms.[89] The results for quenching in the presence of these other metal ions are shown in Figure S37.

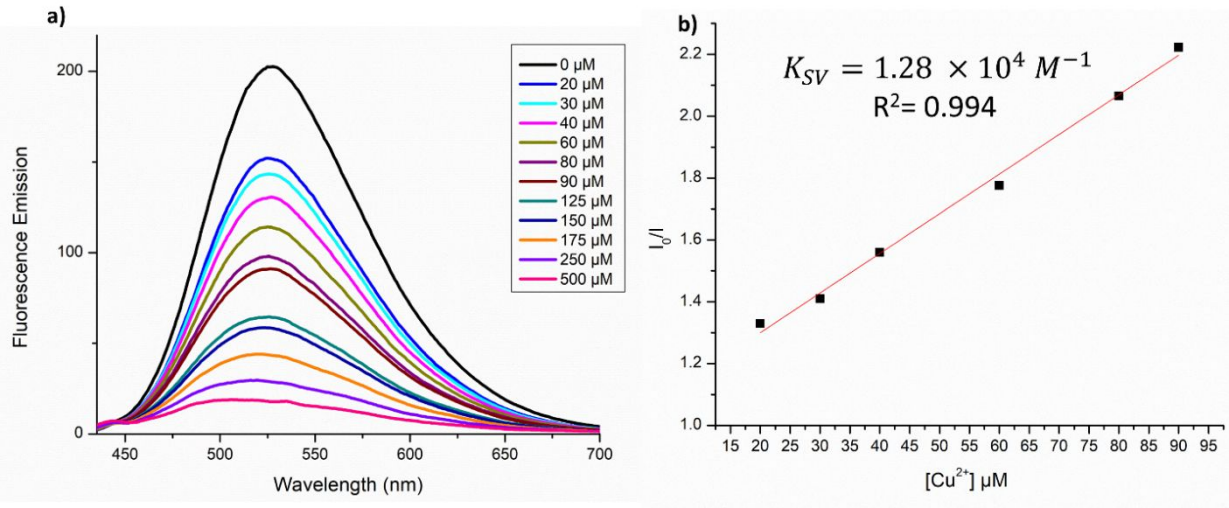

Figure 3. (a) Fluorescence emission of $\mathbf{T_{Ad}}$-*t*$\mathbf{T_{4h}}$ in THF (at a copolymer concentration of 0.01 mg/mL) as a function of the concentration of Cu^{2+}. Although the fluorescence responsiveness persists to much higher concentrations, (b) a linear fluorescence quenching response is observed for $\mathbf{T_{Ad}}$-*t*$\mathbf{T_{4h}}$ at $[Cu^{2+}] \leq 90$ μM.

Reversibility of fluorescence quenching is examined by subjecting the solution, which contains complexes formed by association of pendant adenine groups and Cu^{2+} ions, to a stronger binding ligand, EDTA disodium. As shown in Figure 4, the fluorescence of $\mathbf{T_{Ad}}$-*t*$\mathbf{T_{4h}}$, here at 0.02 mg/mL in chloroform, was recovered almost quantitatively upon washing the solution with excess aqueous solution containing 1 mM EDTA disodium salt. (99% recovery based on intensity measured at λ_{max}^{em}.) The strong multidentate binding offered by EDTA extracts copper ions from the organic phase, resulting in recovery of the fluorescence emission. This reversibility suggests that water soluble adenine-functionalized polythiophenes could be useful as fluorescent probes for biological imaging applications.

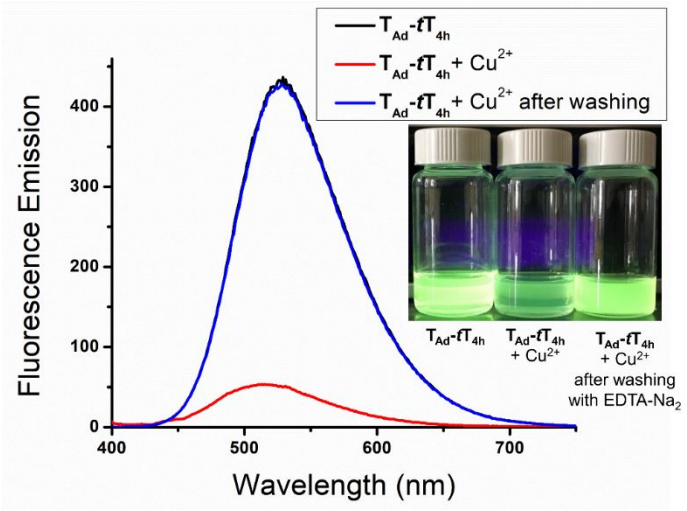

Figure 4. A sequence of measurements demonstrates that fluorescence emission of $\mathbf{T_{Ad}}$-$\mathbf{\textit{t}T_{4h}}$, is quenched upon addition of Cu^{2+} and subsequently recovered after washing with an aqueous EDTA solution.

Conclusions

The efficient synthesis of highly-soluble conjugated polymers with functional groups for site-specific interactions that generate changes in optical properties or control morphological evolution is conceptually important for myriad applications. Here, we used direct arylation polymerization (DArP) to synthesize alternating, thiophene-based copolymers containing adenine functionality in sidechains, which are represented as $\mathbf{T_{Ad}}$-**T** and $\mathbf{T_{Ad}}$-$\mathbf{\textit{t}T_{4h}}$. The use of Boc protection circumvented irreversible binding of the Pd catalyst to the amine group of the adenine pendant along the copolymer backbone, which otherwise prevented polymerization, and the tendency for decreased solubility due to pendant nucleobase functionality was overcome by introducing a terthiophene comonomer with additional solubilizing alkyl side chains. By comparison to an unfunctionalized homolog having the same regioregularity, interchain hydrogen bonding interactions are believed to impact chain packing through the formation of physical network, which manifests as a significant increase the in glass transition temperature. Adenine pendent groups chelate cupric, ferrous, and ferric ions, leading to fast fluorescence quenching that

is triggered by energy transfer from the conjugated polymer main chain to the adenine-copper complex formed upon metal ion binding. The reversible binding enables fluorescence recovery, opening possibilities for metal ion sensing, which paves the way for designing copolymers that may be useful in bio-related applications. Successful utilization of nucleobase-functionalized, conjugated copolymers in various applications will be contingent on balancing functionality with solubility. Therefore, the use of DArP to synthesize adenine-containing copolymers represents a foundational example that motivates future efforts to create functional, conjugated copolymers that offer site-specific interactions afforded by nucleobases, thereby opening new possibilities in sensing and diagnostics, coordination-driven self-assembly, and self-healing materials.

Conflicts of Interest

There are no conflicts to declare.

ORCID IDs

Sina Sabury: 0000-0003-0347-7405

Graham S. Collier: 0000-0002-9650-8110

S. Michael Kilbey II: 0000-0002-9431-1138

Acknowledgements

This work was sponsored in part by the DOE NEET program on ASI, DE-AC05-00OR22725. SS and SMKII acknowledge partial support from the National Science Foundation (Award# 1512221). Oak Ridge National Laboratory is managed by UT-Battelle, LLC, for the Department of Energy under contract DE-AC05-00OR22725.

[†]Footnote

Electronic supplementary information (ESI) available: Synthetic procedures, ^{1}H and ^{13}C NMR spectra of synthesized molecules, GPC elugrams, ^{1}H NMR spectra, TGA and DSC traces, and photophysical properties of synthesized copolymers, behavior over full concentration range used in the fluorescence quenching studies of $\mathbf{T_{Ad}}$-$\boldsymbol{t}\mathbf{T_{4h}}$, and comparison of quenching efficiencies.

References

1. S. Fall, L. Biniek, Y. Odarchenko, D. V. Anokhin, G. de Tournadre, P. Lévêque, N. Leclerc, D. A. Ivanov, O. Simonetti and L. Giraudet, *J. Mater. Chem. C*, 2016, **4**, 286-294.
2. Y. Wang, Y. Liu, S. Chen, R. Peng and Z. Ge, *Chem. Mater.*, 2013, **25**, 3196-3204.
3. J. Mei and Z. Bao, *Chem. Mater.*, 2013, **26**, 604-615.
4. I. Kang, H.-J. Yun, D. S. Chung, S.-K. Kwon and Y.-H. Kim, *J. Am. Chem. Soc.*, 2013, **135**, 14896-14899.
5. L. Li, L. Feng, J. Yuan, H. Peng, Y. Zou and Y. Li, *Chem. Phys. Lett.*, 2018, **696**, 19-25.
6. M. U. Ocheje, B. P. Charron, Y.-H. Cheng, C.-H. Chuang, A. Soldera, Y.-C. Chiu and S. Rondeau-Gagné, *Macromolecules*, 2018, **51**, 1336-1344.
7. T. Prosa, M. Winokur and R. McCullough, *Macromolecules*, 1996, **29**, 3654-3656.
8. C. Cui and W. Y. Wong, *Macromol. Rapid Commun.*, 2016, **37**, 287-302.
9. L. Ye, S. Zhang, W. Zhao, H. Yao and J. Hou, *Chem. Mater.*, 2014, **26**, 3603-3605.
10. R. Kroon, A. Lundin, C. Lindqvist, P. Henriksson, T. T. Steckler and M. R. Andersson, *Polymer*, 2013, **54**, 1285-1288.
11. F. Feng, F. He, L. An, S. Wang, Y. Li and D. Zhu, *Adv. Mater.*, 2008, **20**, 2959-2964.
12. H. J. Kim, M. Pei, J. S. Ko, M. H. Ma, G. E. Park, J. Baek, H. Yang, M. J. Cho and D. H. Choi, *ACS Appl. Mater. Interfaces*, 2018, **10**, 40681-40691.
13. J. H. Dou, Y. Q. Zheng, T. Lei, S. D. Zhang, Z. Wang, W. B. Zhang, J. Y. Wang and J. Pei, *Adv. Funct. Mater.*, 2014, **24**, 6270-6278.
14. Z. Xiao, T. Duan, H. Chen, K. Sun and S. Lu, *Sol. Energy Mater. Sol. Cells*, 2018, **182**, 1-13.
15. C.-C. Cheng, Y.-L. Chu, P.-H. Huang, Y.-C. Yen, C.-W. Chu, A. C.-M. Yang, F.-H. Ko, J.-K. Chen and F.-C. Chang, *J. Mater. Chem.*, 2012, **22**, 18127-18131.
16. T. Aytun, L. Barreda, A. Ruiz-Carretero, J. A. Lehrman and S. I. Stupp, *Chem. Mater.*, 2015, **27**, 1201-1209.
17. D. W. Bilger, J. A. Figueroa, N. D. Redeker, A. Sarkar, M. Stefik and S. Zhang, *ACS Omega*, 2017, **2**, 8526-8535.
18. J. Yao, C. Yu, Z. Liu, H. Luo, Y. Yang, G. Zhang and D. Zhang, *J. Am. Chem. Soc.*, 2015, **138**, 173-185.
19. C. Xing, H. Yuan, S. Xu, H. An, R. Niu and Y. Zhan, *ACS Appl. Mater. Interfaces*, 2014, **6**, 9601-9607.
20. X. Feng, L. Liu, S. Wang and D. Zhu, *Chem. Soc. Rev.*, 2010, **39**, 2411-2419.
21. E. S. Baker, J. W. Hong, B. S. Gaylord, G. C. Bazan and M. T. Bowers, *J. Am. Chem. Soc.*, 2006, **128**, 8484-8492.
22. X. Liu, L. Ouyang, X. Cai, Y. Huang, X. Feng, Q. Fan and W. Huang, *Biosens. Bioelectron.*, 2013, **41**, 218-224.
23. X. Liu, Q. Fan and W. Huang, *Biosens. Bioelectron.*, 2011, **26**, 2154-2164.
24. Y. Lu, X. Li, G. Wang and W. Tang, *Biosens. Bioelectron.*, 2013, **39**, 231-235.
25. B. Liu and G. C. Bazan, *Chem. Mater.*, 2004, **16**, 4467-4476.
26. Y. Tang, F. He, M. Yu, F. Feng, L. An, H. Sun, S. Wang, Y. Li and D. Zhu, *Macromol. Rapid Commun.*, 2006, **27**, 389-392.
27. A.-I. Gopalan, S. Komathi, N. Muthuchamy, K. P. Lee, M. J. Whitcombe, D. Lakshmi and G. Sai-Anand, *Prog. Polym. Sci.*, 2018.
28. P. Bäuerle and A. Emge, *Adv. Mater.*, 1998, **10**, 324-330.
29. S. Sivakova and S. J. Rowan, *Chem. Soc. Rev.*, 2005, **34**, 9-21.

30. R. Leist, J. A. Frey, P. Ottiger, H. M. Frey, S. Leutwyler, R. A. Bachorz and W. Klopper, *Angew. Chem.*, 2007, **119**, 7593-7596.
31. H. Yang and W. Xi, *Polymers*, 2017, **9**, 666.
32. S. Cheng, M. Zhang, N. Dixit, R. B. Moore and T. E. Long, *Macromolecules*, 2012, **45**, 805-812.
33. R. E. Kleiner, Y. Brudno, M. E. Birnbaum and D. R. Liu, *J. Am. Chem. Soc.*, 2008, **130**, 4646-4659.
34. Z. Hua, T. R. Wilks, R. Keogh, G. Herwig, V. G. Stavros and R. K. O'Reilly, *Chem. Mater.*, 2018, **30**, 1408-1416.
35. F. Li, N. M. Dawson, Y.-B. Jiang, K. J. Malloy and Y. Qin, *Polymer*, 2015, **76**, 220-229.
36. Y. Z. Yang, Z. T. Liu, L. L. Chen, J. J. Yao, G. B. Lin, X. S. Zhang, G. X. Zhang and D. Q. Zhang, *Chem. Mater.*, 2019, **31**, 1800-1807.
37. B. Lippert, *Coord. Chem. Rev.*, 2000, **200**, 487-516.
38. C.-C. Cheng, F.-C. Chang, F.-H. Ko, F.-C. Yu, Y.-T. Lin, Y.-T. Shieh, J.-K. Chen and D.-J. Lee, *J. Mater. Chem. C*, 2015, **3**, 9528-9533.
39. M. S. Abdou, X. Lu, Z. W. Xie, F. Orfino, M. J. Deen and S. Holdcroft, *Chem. Mater.*, 1995, **7**, 631-641.
40. D. Vangeneugden, D. Vanderzande, J. Salbeck, P. Van Hal, R. Janssen, J. Hummelen, C. Brabec, S. Shaheen and N. Sariciftci, *The Journal of Physical Chemistry B*, 2001, **105**, 11106-11113.
41. C. G. Fraga, *Molecular aspects of medicine*, 2005, **26**, 235-244.
42. C.-C. Cheng, J.-K. Chen, Y.-T. Shieh and D.-J. Lee, *Nanotechnology*, 2016, **27**, 32LT01.
43. R. M. Pankow, L. W. Ye, N. S. Gobalasingham, N. Salami, S. Samal and B. C. Thompson, *Polym. Chem.*, 2018, **9**, 3885-3892.
44. T. Bura, J. T. Blaskovits and M. Leclerc, *J. Am. Chem. Soc.*, 2016, **138**, 10056-10071.
45. X. Wang, K. Wang and M. Wang, *Polym. Chem.*, 2015, **6**, 1846-1855.
46. S. Hayashi, Y. Kojima and T. Koizumi, *Polym. Chem.*, 2015, **6**, 881-885.
47. N. S. Gobalasingham, S. Ekiz, R. M. Pankow, F. Livi, E. Bundgaard and B. C. Thompson, *Polym. Chem.*, 2017, **8**, 4393-4402.
48. L. G. Mercier and M. Leclerc, *Acc. Chem. Res.*, 2013, **46**, 1597-1605.
49. L. A. Estrada, J. J. Deininger, G. D. Kamenov and J. R. Reynolds, *ACS Macro Lett.*, 2013, **2**, 869-873.
50. L. Zhai, R. L. Pilston, K. L. Zaiger, K. K. Stokes and R. D. McCullough, *Macromolecules*, 2003, **36**, 61-64.
51. E. F. Palermo, H. L. van der Laan and A. J. McNeil, *Polym. Chem.*, 2013, **4**, 4606-4611.
52. C. Lambertucci, I. Antonini, M. Buccioni, D. Dal Ben, D. D. Kachare, R. Volpini, K.-N. Klotz and G. Cristalli, *Bioorg. Med. Chem.*, 2009, **17**, 2812-2822.
53. G. S. Collier, L. A. Brown, E. S. Boone, B. K. Long and S. M. Kilbey, *ACS Macro Lett.*, 2016, **5**, 682-687.
54. G. S. Collier, L. A. Brown, E. S. Boone, M. Kaushal, M. N. Ericson, M. G. Walter, B. K. Long and S. M. Kilbey, *J. Mater. Chem. C*, 2017, **5**, 6891-6898.
55. A. K. Mishra, R. K. Prajapati and S. Verma, *Dalton Trans.*, 2010, **39**, 10034-10037.
56. D. Dal Ben, M. Buccioni, C. Lambertucci, A. Thomas, K.-N. Klotz, S. Federico, B. Cacciari, G. Spalluto and R. Volpini, *Eur. J. Med. Chem.*, 2013, **70**, 525-535.
57. C. Fonseca Guerra, F. Bickelhaupt, S. Saha and F. Wang, *J. Phys. Chem. A*, 2006, **110**, 4012-4020.
58. A. E. Rudenko, C. A. Wiley, J. F. Tannaci and B. C. Thompson, *J. Polym. Sci., Part A: Polym. Chem.*, 2013, **51**, 2660-2668.
59. A. E. Rudenko and B. C. Thompson, *J. Polym. Sci., Part A: Polym. Chem.*, 2015, **53**, 135-147.
60. I. Cerna, R. Pohl, B. Klepetarova and M. Hocek, *J. Org. Chem.*, 2008, **73**, 9048-9054.
61. P. Štarha, R. Novotná and Z. Trávníček, *Inorg. Chem. Commun.*, 2010, **13**, 800-803.
62. Z. Szabó, *Coord. Chem. Rev.*, 2008, **252**, 2362-2380.

63. B. Lippert, *J. Chem. Soc., Dalton Trans.*, 1997, 3971-3976.
64. J. Sponer, M. Sabat, L. Gorb, J. Leszczynski, B. Lippert and P. Hobza, *J. Phys. Chem. B*, 2000, **104**, 7535-7544.
65. A. Bhattacharya and A. De, *Journal of Macromolecular Science, Part C*, 1999, **39**, 17-56.
66. P.-T. Wu, G. Ren and S. A. Jenekhe, *Macromolecules*, 2010, **43**, 3306-3313.
67. Y. Lee, M. P. Aplan, Z. D. Seibers, R. Xie, T. E. Culp, C. Wang, A. Hexemer, S. M. Kilbey, Q. Wang and E. D. Gomez, *Macromolecules*, 2018, **51**, 8844-8852.
68. M. Rehahn, A. D. Schlüter and G. Wegner, *Makromol. Chem.*, 1990, **191**, 1991-2003.
69. A. Rodrigues, M. C. R. Castro, A. S. Farinha, M. Oliveira, J. P. Tomé, A. V. Machado, M. M. M. Raposo, L. Hilliou and G. Bernardo, *Polym. Test.*, 2013, **32**, 1192-1201.
70. C.-C. Cheng, Y.-L. Chu, F.-C. Chang, D.-J. Lee, Y.-C. Yen, J.-K. Chen, C.-W. Chu and Z. Xin, *Nano Energy*, 2015, **13**, 1-8.
71. S. W. Kuo, H. Xu, C. F. Huang and F. C. Chang, *J. Polym. Sci., Part B: Polym. Phys.*, 2002, **40**, 2313-2323.
72. A. Kraft, A. C. Grimsdale and A. B. Holmes, *Angew. Chem. Int. Ed.*, 1998, **37**, 402-428.
73. H. H. Hammud, K. H. Bouhadir, M. S. Masoud, A. M. Ghannoum and S. A. Assi, *J. Solution Chem.*, 2008, **37**, 895.
74. S. Domínguez, M. Cangiotti, A. Fattori, T. Ääritalo, P. Damlin, M. Ottaviani and C. Kvarnström, *Langmuir*, 2018, **34**, 7364-7378.
75. A. C. Grimsdale, K. Leok Chan, R. E. Martin, P. G. Jokisz and A. B. Holmes, *Chem. Rev.*, 2009, **109**, 897-1091.
76. I. F. Perepichka, D. F. Perepichka, H. Meng and F. Wudl, *Adv. Mater.*, 2005, **17**, 2281-2305.
77. O. P. Dimitriev, D. A. Blank, C. Ganser and C. Teichert, *J. Phys. Chem. C*, 2018, **122**, 17096-17109.
78. J. R. Lakowicz, *Principles of fluorescence spectroscopy*, Springer Science & Business Media, 2013.
79. T. Karstens and K. Kobs, *The journal of physical chemistry*, 1980, **84**, 1871-1872.
80. S. Cook, A. Furube and R. Katoh, *Energy Environ. Sci.*, 2008, **1**, 294-299.
81. J. Piris, T. E. Dykstra, A. A. Bakulin, P. H. v. Loosdrecht, W. Knulst, M. T. Trinh, J. M. Schins and L. D. Siebbeles, *J. Phys. Chem. C*, 2009, **113**, 14500-14506.
82. N. P. Wells, B. W. Boudouris, M. A. Hillmyer and D. A. Blank, *J. Phys. Chem. C*, 2007, **111**, 15404-15414.
83. B. Xu and S. Holdcroft, *Macromolecules*, 1993, **26**, 4457-4460.
84. A. O. Weldeab, L. Li, S. Cekli, K. A. Abboud, K. S. Schanze and R. K. Castellano, *Org. Chem. Front.*, 2018, **5**, 3170-3177.
85. A. Casey, R. S. Ashraf, Z. Fei and M. Heeney, *Macromolecules*, 2014, **47**, 2279-2288.
86. T. Dutta, K. B. Woody, S. R. Parkin, M. D. Watson and J. Gierschner, *J. Am. Chem. Soc.*, 2009, **131**, 17321-17327.
87. L.-J. Fan, Y. Zhang, C. B. Murphy, S. E. Angell, M. F. Parker, B. R. Flynn and W. E. Jones Jr, *Coord. Chem. Rev.*, 2009, **253**, 410-422.
88. L. Wenfeng, M. Hengchang, M. Yuan, Q. Chunxuan, Z. Zhonwei, Y. Zengming and C. Haiying, *RSC Adv.*, 2015, **5**, 6869-6878.
89. M. Formica, V. Fusi, L. Giorgi and M. Micheloni, *Coord. Chem. Rev.*, 2012, **256**, 170-192.
90. L. K. Fraiji, D. M. Hayes and T. Werner, *J. Chem. Educ.*, 1992, **69**, 424.

TOC Graphic

Synthesis of a Soluble Adenine-Functionalized Polythiophene through Direct Arylation Polymerization and its Fluorescence Responsive Behavior

Sabury et al.

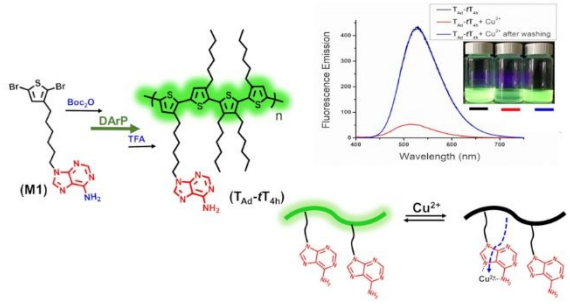

Statement to accompany TOC (limited to 250 characters):

An adenine-functionalized, thiophene-based alternating copolymer is synthesized via direct arylation polymerization using Boc-protection to overcome catalyst-adenine complexation. The nucleobase-tagged copolymer is highly soluble and displays reversible fluorescence quenching.